AEROSOLS FOR CONCENTRATING SOLAR ELECTRICITY PRODUCTION FORECASTS

Requirement Quantification and ECMWF/MACC Aerosol Forecast Assessment

BY MARION SCHROEDTER-HOMSCHEIDT, ARMEL OUMBE, ANGELA BENEDETTI, AND JEAN-JACQUES MORCRETTE

Extending numerical weather forecasting with chemical weather modeling will improve prediction of aerosol extinction and direct irradiance at the surface—and thus increase reliability of solar energy.

USER REQUIREMENTS FROM THE SOLAR SECTOR. Concentrating solar power (CSP) systems use lenses or mirrors and tracking systems to focus a large area of sunlight onto a small area. A working fluid is heated by the concentrated sunlight, and this thermal energy can be stored or immediately used to produce electricity via a steam turbine. Alternatively, concentrating photovoltaics (CPV) are a future technology with growing interest among industries, where sunlight is concentrated on smaller and highly efficient but rather expensive photovoltaic cells. Concentrating technologies utilize direct normal irradiance (DNI), which is the direct irradiance on the normal plane with respect to the incoming beam. Typically, DNI is measured as the incoming irradiance from the Sun's disc together with circumsolar diffuse irradiance within a cone of 2.5° around the Sun's center (WMO 2010).

Sunlight is the fuel for each solar energy conversion system. Like any generation source, knowledge about the fuel's quality and future reliability is essential for an accurate estimate of technical system performance and financial viability of a project. For site selection, choosing the optimum energy conversion technology, or designing systems for specific locations, it is necessary to understand the long-term spatial and temporal variability of available solar resources. For these applications long-term annual or monthly irradiation sums together with accurate frequency distributions of solar irradiance are needed and provided with the help of satellite data (Cano et al. 1986; Beyer et al. 1996; Rigollier et al. 2004). However, short- and medium-term forecasts of the solar resource will remain essential to the plant's efficient operations and its integration into the electricity grid throughout its lifetime.

It has to be noted that users from the nonconcentrating photovoltaic technology sector require a high global irradiance forecast accuracy. This can mainly be achieved through high cloud forecast accuracy, while aerosols are of only minor importance for this purpose. On the other hand, users from the CSP sector need a high DNI forecast accuracy especially in cloud-free cases with high DNI. Additionally, CSP users request a good forecast on the occurrence of low DNI cases—which refers mainly to a good water cloud mask forecast—and a good forecast of medium DNI cases—which refers to the cirrus cloud optical properties forecast. CSP technologies generally operate only in areas with high DNI and small cloud cover. Therefore, depending on the geographical region of interest and its vicinity to global aerosol sources, the priority is set either on good aerosol or cirrus forecasts. This paper focuses on the aerosol forecast accuracy, while assessing the requirements on cirrus clouds and the modeling capabilities in today's NWP would be a separate subject.

CSP electrical energy production can be calculated by using a power plant model and DNI as an input parameter. The power plant model has to simulate

the thermal state of the heat transfer fluid and its pumping through the solar field; the hot and cold heat storage tank's status; heat exchangers used between the solar field, tanks, and the turbine; technical turbine specifics; and, finally, a model of the manual and interactive control of the power plant by its operator team (e.g., Wittmann et al. 2008; Klein et al. 2010; Wagner and Gilman 2011).

The strong dependency between DNI and CSP electricity production makes forecasting of direct solar irradiance essential (Pulvermüller et al. 2009; Wittmann et al. 2008). In the Spanish electricity market, for example, the hourly electrical energy production forecast for a given day has to be delivered on the previous day before 1000 LT (Ministerio de Industria, Turismo y Comercio 2007). A high-quality forecasting system reduces the power plant operator's risk of penalty payments due to inaccurate production forecasts and helps the transmission grid operator to keep operations stable. According to the Spanish regulation, penalties apply to cover additional costs occurring for the electricity grid operator in case of inaccurate electricity production forecasts provided by the power plant operator. For example, in case of a lower production than predicted in a certain hour of the day, the electricity grid operator might need to purchase additional electricity from other sources on the short-term electricity market. These extra costs can be forwarded to the power plant operator as a penalty. Penalties may apply if production forecasts are too small—resulting in additional purchase needs—or too high—resulting in additional selling needs at the grid operator's side. Penalties apply only if costs occurred in reality—for example, a lower production than predicted, which occurs in a situation with lower electricity consumption than predicted, might not cause any additional purchase needs and therefore no costs.

Kraas et al. (2010, 2011) analyzed how a good DNI forecast can enhance the profitability of a power plant when operating at a day-ahead electricity market. In their case study for a power plant in southern Spain, a relative DNI forecasting error magnitude of 10%–20% and 20%–30% respectively led to €1.5 $(MWh)^{-1}$ and €2.5 $(MWh)^{-1}$ penalties in a reference year based on actual market conditions. A 10% improvement in forecasting leads to a penalty reduction of about 7%. Additionally, an accurate production forecast can increase plant profits by optimizing energy dispatch into the time periods of greatest value on the electricity markets.

The current state of the art in NWP provides rather inaccurate DNI forecasts. Lara-Fanego et al. (2012) found a relative RMSE of 60% for hourly DNI forecasts in Spain using an Advanced Research Weather Research and Forecasting model (ARW-WRF) (version 3) model implementation for all sky conditions (cloudy as well as cloud free). In overcast skies, knowledge of cloud cover and type is most important. Nevertheless, in high solar resource regions as the Mediterranean and northern Africa, because less cloudy aerosol loading is the most critical atmospheric parameter since up to 30% of additional direct irradiance extinction have been reported (e.g., Wittmann et al. 2008). In dust outbreak events, the extinction of DNI reaches even up to 100%. Breitkreuz et al. (2009) compared direct irradiances calculated from Aerosol Robotic Network (AERONET) measurements, the European Centre for Medium-Range Weather Forecasts (ECMWF) operational model, and forecasted aerosol optical depth (AOD) of the European Dispersion and Deposition model (EURAD)-based AOD forecasts in order to quantify the effects of varying AOD forecast quality on solar energy applications. They show that a chemical transport model designed for air quality research is strongly needed for solar irradiance forecasting in clear-sky conditions. It improves the relative RMSE from 31% to 19% in clear-sky conditions.

As part of the Monitoring Atmospheric Composition and Climate (MACC) project within the European Union's Global Monitoring of Environment and Security (GMES) program, the ECMWF Integrated Forecast System (IFS) has recently been modified to include a chemical weather prediction suite, which provides an analysis and subsequent forecast of aerosols (Benedetti et al. 2009; Morcrette

AFFILIATIONS: Schroedter-Homscheidt—German Aerospace Center (DLR), Earth Observation Center, Oberpfaffenhofen, Germany; Oumbe*—Deutsches Zentrum für Luft- und Raumfahrt (DLR), Earth Observation Center, Oberpfaffenhofen, Germany; Benedetti and Morcrette—European Centre for Medium-Range Weather Forecasts, Data Assimilation Section, Reading, United Kingdom
*** CURRENT AFFILIATION:** Total New Energies, R&D–Concentrated Solar Technologies, Courbevoie, France
CORRESPONDING AUTHOR: Dr. Marion Schroedter-Homscheidt, German Aerospace Center (DLR), Earth Observation Center, 82234 Oberpfaffenhofen, Germany
E-mail: marion.schroedter-homscheidt@dlr.de

The abstract for this article can be found in this issue, following the table of contents.
DOI:10.1175/BAMS-D-11-00259.1

In final form 28 August 2012

et al. 2009, 2011). This opens the field for improved NWP-based DNI forecasts by using an operational aerosol forecast.

The objectives of this paper are to quantify the accuracy and temporal resolution needed for AOD forecasts with respect to hourly DNI forecasts. This includes the questions of whether and where a daily mean forecast or a 2-day persistence approach might be sufficient. Finally, MACC AOD forecasts are assessed and compared versus the 2-day persistence approach in order to give a first impression as to whether the recently introduced aerosol modeling in NWP centers is already applicable for the solar user community.

AERONET AOD MEASUREMENTS USED. Ground-based sun photometer measurements made in the AERONET network are used as reference for each forecast validation and for estimating the intra-day AOD variation at 550 nm. The accuracy of AOD values is ±0.01 for wavelengths larger than 440 nm (Holben et al. 1998). In this study, all 537 level 2.0 (cloud screened and quality assured) AERONET stations operating during any phase inside the period August 1992 to January 2011 are used. The exact period of measurements changes from a few months corresponding to a particular campaign to years for each station. All AERONET measurements within an hour are used to create hourly mean values. A station is considered only if there are at least 100 matching hours. The availability of only clear-sky and daytime observations is well suited to assess a parameter relevant for concentrating solar energy applications, as they operate mainly in the same conditions.

ECMWF/MACC AEROSOL FORECAST. The Global and Regional Earth-System Monitoring Using Satellite and in Situ Data (GEMS) project developed the capability of modeling atmospheric constituents such as aerosols, greenhouse, and reactive gases within the ECMWF. This prognostic aerosol scheme has been used in the ECMWF IFS in both its analysis and forecast modules to provide a reanalysis and a near-real-time (NRT) run. Five types of tropospheric aerosols are considered: sea salt, dust, organic and black carbon, and sulfate. The two natural aerosols sea salt and dust have their sources linked to prognostic and diagnostic surface and near-surface model variables. In contrast, organic matter, black carbon, and sulfate have their external source databases. Physical processes as dry deposition, including the turbulent transfer and gravitational settling to the surface, and wet deposition, including rainout and washout of aerosol particles in and below the clouds, are considered. Moderate Resolution Imaging Spectroradiometer (MODIS) observations of AOD at 550 nm from collection 5 and 6 (Remer et al. 2005) from both the *Terra* and *Aqua* satellites are assimilated in the ECMWF operational four-dimensional assimilation system (Rabier et al. 2000; Mahfouf and Rabier 2000; Klinker et al. 2000). A more detailed description of the MACC NRT run is found in Morcrette et al. (2009, 2011) and Benedetti et al. (2009). ECMWF/MACC AOD 550-nm forecasts in 3-hourly resolution with forecast duration of 48 h were obtained on a reduced N80 Gaussian grid with a resolution of 1.125° in latitudes. At the time of this study ECMWF/MACC data had been available for the period September 2009 to December 2010. Since measurements at some AERONET stations originate from a short-term campaign, and because of the delay in the availability of quality-controlled level 2.0 data, there are fewer stations available for ECMWF/MACC validations than for pure AERONET-based assessments.

ASSESSMENT METHOD. The classical approach of comparing measured and forecasted AOD time series would be to investigate differences in AOD (ΔAOD, marked with a red symbol in Fig. 1). In this study, we are interested in errors in DNI caused by a ΔAOD at an individual hour of the day—Fig. 1 illustrates the assessment method used. A ΔAOD generates a different ΔDNI for high and low aerosol loadings, and ΔDNI also depends on the solar zenith angle and the aerosol type (Fig. 2, details explained below). Therefore, hours with a ΔAOD being greater

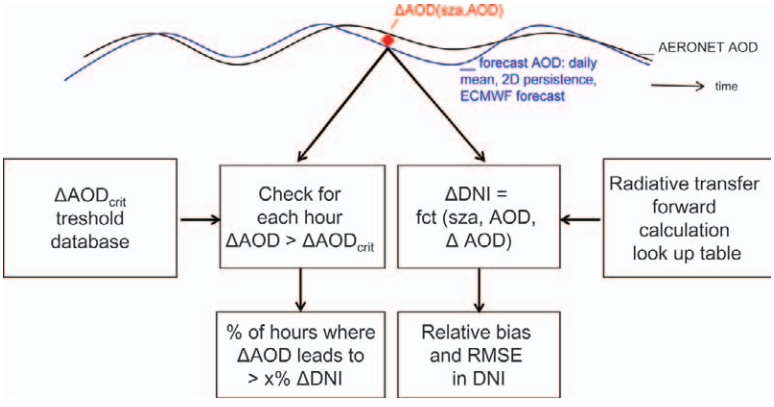

Fig. 1. Scheme of AOD forecast assessment with respect to DNI forecast accuracy and using a ΔAOD$_{crit}$ thresholds database.

than a critical AOD difference (ΔAOD_{crit}) are counted. Values ΔAOD_{crit} are defined as the threshold when a more than x% DNI deviation is caused by the actual ΔAOD with respect to solar position and the AOD value itself. This results in the user-specific exceedance hour parameter, which corresponds to the percentage of hours when an AOD deviation leads to at least a 5%, 10%, or 20% DNI deviation. Such a probability of exceedance can be used in economic assessments more easily than any ΔAOD information. Additionally, ΔDNI is derived from ΔAOD generating standard parameters as the relative bias and the relative root mean square deviation (RMS).

The solar sector does not provide a single number of an acceptable maximum hourly DNI deviation as the acceptable DNI forecast accuracy is dependent on the economic viability of a power plant. This depends on many, partly time-varying factors such as the electricity market prices, loan conditions for investors, regulation requirements from national authorities, the potential return on investment for alternative investments, and, last but not least, the concentrating solar technology chosen among a variety of technology options. Therefore, this paper provides results for different ΔDNI ranges and assumes that a power plant developer will use the results being appropriate for a specific solar power plant project development.

For the derivation of ΔAOD_{crit} thresholds and for all solar surface irradiance calculations, the radiative transfer model Library for Radiative Transfer (LibRadtran; Mayer and Kylling 2005) with its solver Discrete Ordinate Radiative Transfer model (DISORT) (Stamnes et al. 1988) is used. Its accuracy has, for example, been demonstrated in Kylling et al. (2005). Since CSP systems use the complete solar spectrum, only the broadband direct irradiance is

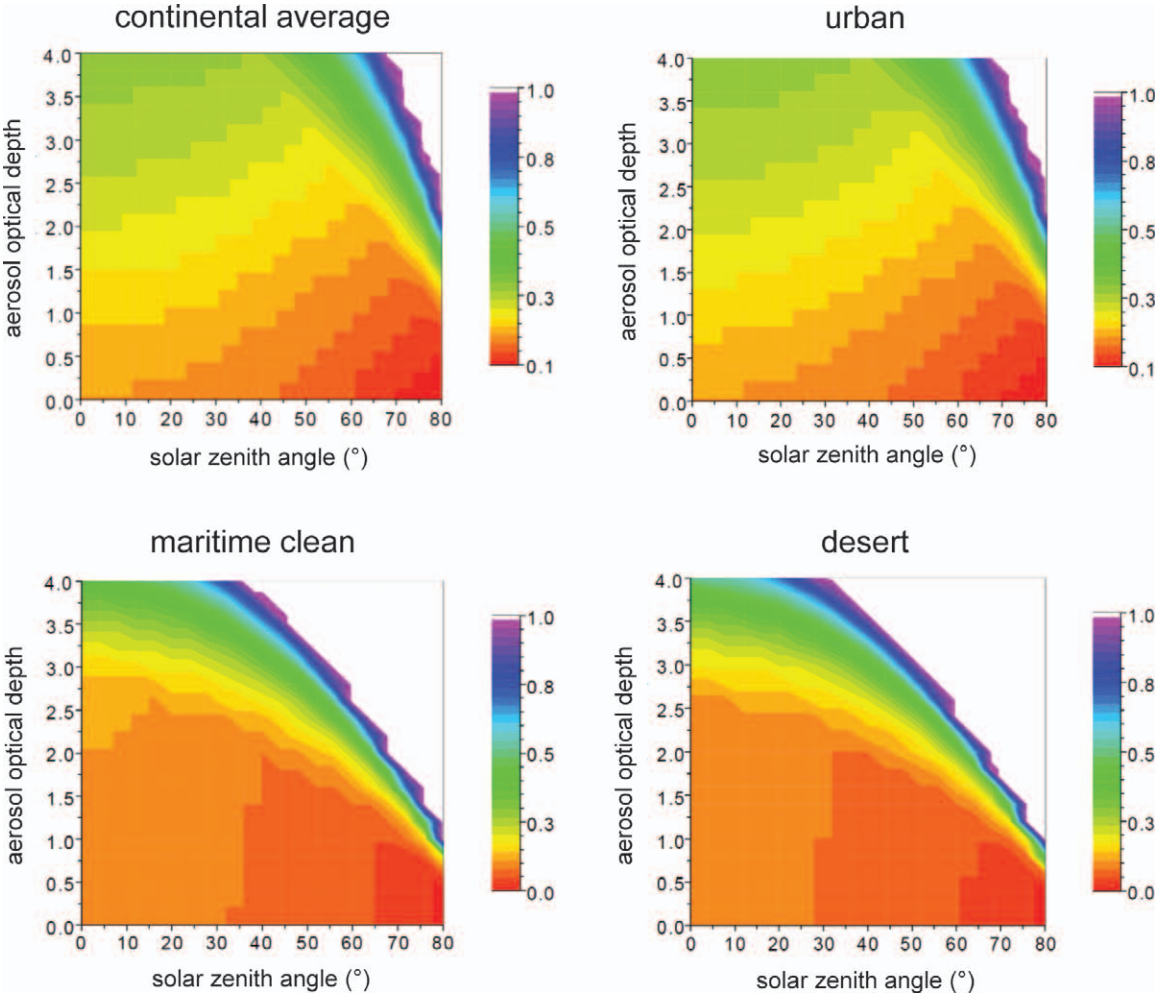

Fig. 2. Variation of critical AOD deviation with the actual AOD and solar zenith angle. A critical AOD deviation as leading to a 10% DNI deviation is defined in this example. Panels show results for "continental average," "urban," "maritime clean," and "desert" OPAC aerosol types. AOD deviation is set to 1 for a better readability if it is higher than 1, which corresponds to very low DNI.

of interest and transferred towards DNI by using the cosine of the Sun zenith angle (SZA). Values of ΔAOD_{crit} are estimated (Fig. 2) for various AODs, for the four Optical Properties of Aerosols and Clouds (OPAC; Hess et al. 1998) aerosol types used, and varying SZA. By requiring a minimal 10 W m^{-2} ΔDNI, very small DNI values are excluded. The generation of this database acts as a prerequisite to derive the paper's statistical results in the next chapters. Generally, ΔAOD_{crit} is increasing with the AOD, while for small AOD, ΔAOD_{crit} is decreasing with larger SZA reflecting the larger air mass. On the other hand, for high AOD, ΔAOD_{crit} strongly increases with SZA owing to the anyhow large extinction of irradiance. As the surface irradiance at such AOD values gets small, the required minimum deviation of 10 W m^{-2} is more difficult to reach, resulting in this increase of the threshold with SZA.

It has to be noted that the DISORT solver treats the Sun as a point source and therefore neglects circumsolar radiation as seen by a pyrheliometer with a typical half-field of view of 2.5°. Therefore, DNI in this study is not exactly the DNI value as measured with standard pyrheliometers. Generally, this effect is small in the aerosol case, while it becomes an up to 50% effect on the transmittance in the case of cirrus clouds (e.g., Shiobara and Asano 1994; Thomalla et al. 1983). This cirrus effect is neglected assuming that the AERONET level-2 observations are successfully cloud corrected.

Both AERONET and ECMWF/MACC forecasts provide spectral AOD describing the aerosol type implicitly. In LibRadtran calculations, preset aerosol types based on OPAC are used. This assumption is certainly not true for each individual hour, but simplifies the approach. Additionally, this study is performed for CSP technologies exploiting broadband direct irradiances and, therefore, being not as sensitive to the aerosol type as, for example, future thin film photovoltaic technologies. Therefore, details of the ECMWF/MACC aerosol type characterization resulting in spectral AOD errors are also outside the focus of this study. The OPAC aerosol type "continental average" is used at most stations. Cities with more than 2 million inhabitants are marked as urban (29 stations). Stations listed by Huneeus et al. (2011) as dusty are considered as having a desert aerosol type (23 stations). Finally, a visual selection of maritime aerosol type for stations close to the sea or on small isolated islands is made (26 stations). Lists of aerosol urban type, desert type and maritime type stations are given in the appendix.

In this paper we concentrate on requirements for aerosol forecasts. Therefore, all comparisons assume that DNI is only sensitive to aerosol loading. Aerosol loading is the most significant input parameter in clear skies, but depending on SZA and aerosol loading itself, the influence of other atmospheric parameters can be more or less important. A sensitivity study based on randomly selected 50 variations of aerosol Angstrom exponent, total column water vapor, total column ozone, altitude of the ground, ground albedo, and atmospheric profile is made. For each tuple of AOD, aerosol type, and SZA used in Fig. 2, the relative RMS in computed (Fig. 3, left). The influence of other parameters changes with the amount of AOD.

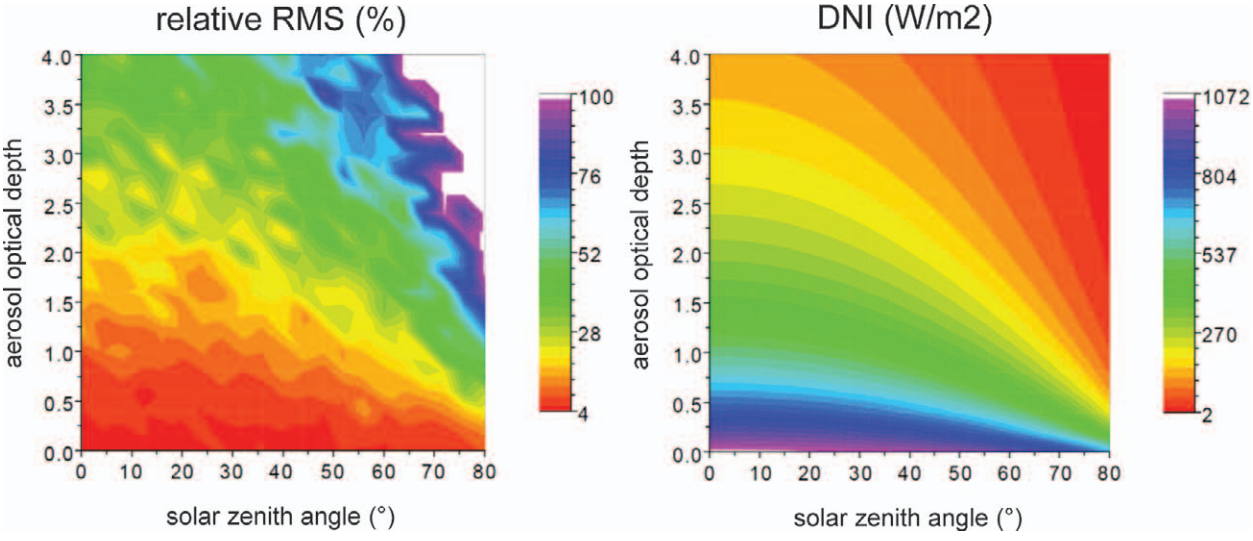

Fig. 3. Relative RMS on DNI due to atmospheric parameters other than AOD and SZA. These plots correspond to the continental average type. Similar results are obtained for other types.

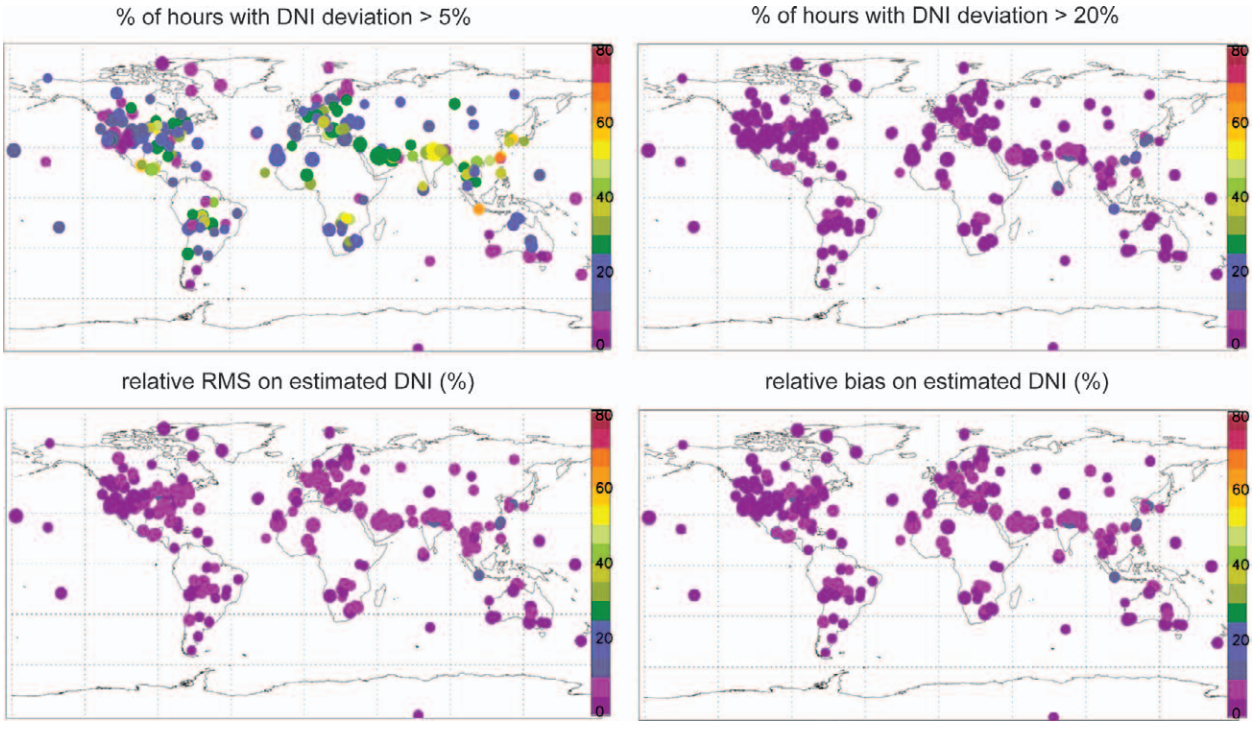

Fig. 4. DNI deviation due to intra-day AOD variation in the AERONET network. The maximum number of days is 2,572, the minimum is 103, and the disk size is proportional to (1 + number of days/maximum number). Each day has at least 10 observations.

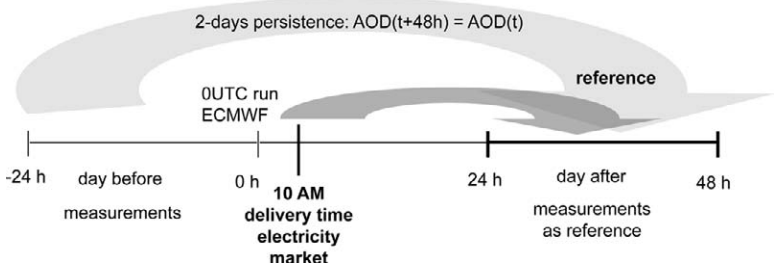

Fig. 5. Overview of AOD forecast timelines—the delivery time here corresponds to the Spanish electricity market.

This deviation can be very large in highly turbid conditions, reaching even extreme values higher than 50%. This occurs only in conditions with DNI less than 200 W/m^2 (Fig. 3, right), which are not relevant for concentrating solar technologies.

IS A DAILY MEAN FORECAST SUFFICIENT?

It has been discussed whether the use of a daily AOD forecasts is sufficient for a DNI forecast in some regions of the world. Therefore, the ΔDNI due to intra-day AOD variation is quantified at the location of each AERONET station (Fig. 4) by comparing AERONET-derived daily AOD means versus hourly means in each forecast hour. In general, the intra-day variation of AOD leads to a small ΔDNI. In most stations, the percentage of hours with a ΔAOD leading to more than 20% ΔDNI is less than 10%. For the stricter criterion of a more than 5% ΔDNI, around 30% of exceedance hours are found in the Europe, Mediterranean, and northern Africa (EUMENA) region and northern America and 60% in Southeast Asia. The mean relative bias and RMS in DNI are rather low, having values generally less than 10%.

A daily cycle with higher ΔDNI at low solar elevations and smaller values in the middle of the day is found. Therefore, the influence of the AOD intra-day variation on DNI is less important when there is more solar resource available during noon hours. Additionally, deviations are generally higher for urban and desert aerosol type dominated stations as they have a larger variability in AOD.

PERFORMANCE OF A 2-DAY PERSISTENCE FORECAST AS POOR MAN'S APPROACH.

Typically, it is required in an electricity production system to deliver the day-ahead energy production forecast of a power plant during morning hours—for example, before 1000 LT in the Spanish

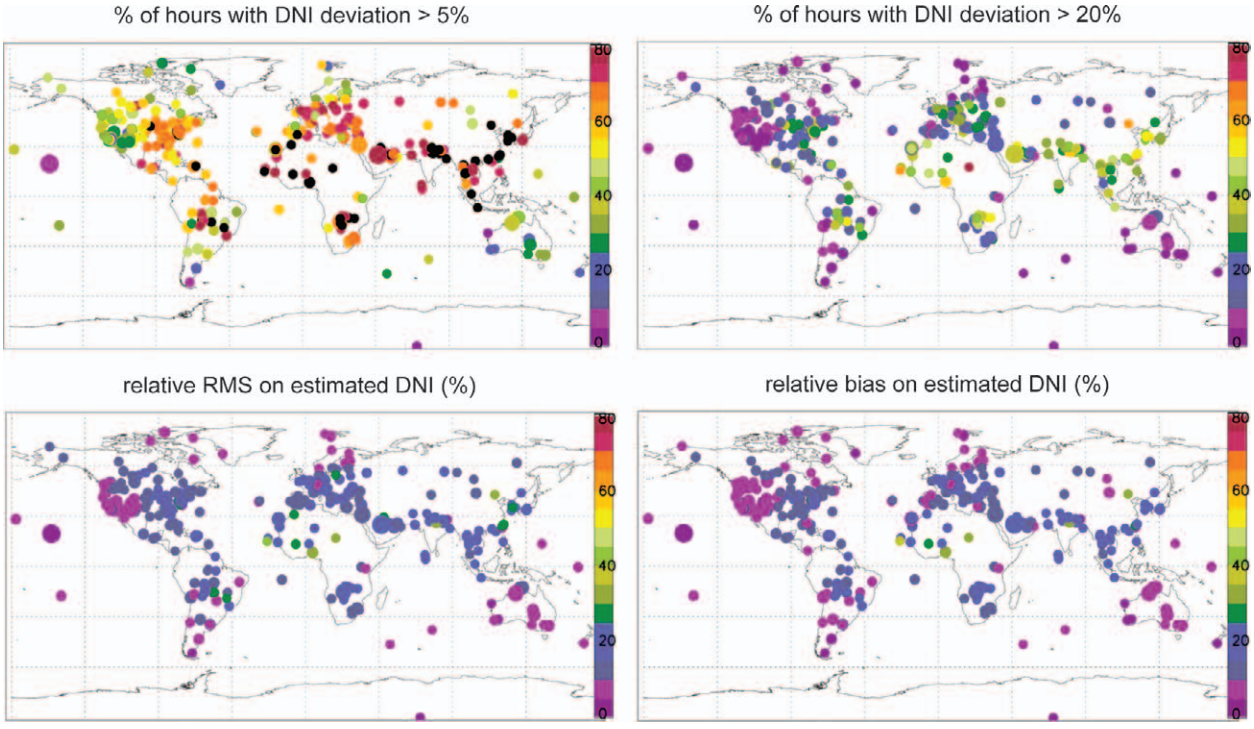

Fig. 6. Two-day persistence assessment at AERONET station locations. The maximum number of hours is 107,635, the minimum is 101, and the disk size is proportional to (1 + number of hours/maximum number). Black points correspond to deviations higher than 80%.

case. Therefore, a 2-day persistence—defined as AOD(t + 48) being equal to AOD(t) for each hourly mean AERONET value (Fig. 5)—is assessed instead of a standard 1-day persistence. The persistence acts both as a potential poor man's approach as well as a reference case for each other forecasting approach (next section).

The relative ΔDNI tends to increase with the mean AOD: Large exceedance hour values are obtained in the Middle East and Southeast Asia for the 20% criterion, while a large number of exceedance hours is also recorded in African areas close to source areas (Fig. 6). Minima are obtained in Australia and northern America (around 10%) and maxima in Southeast Asia and south of the Sahara (around 70%). A similar result is found for exceedance hours owing to a 2-day persistence for the 5% DNI deviation threshold, with an obviously higher percentage of exceeding cases: 70% for EUMENA and the east of northern America and 90% for Southeast Asia and regions close to African deserts. Generally, a 2-day persistence of hourly AOD is not accurate enough for DNI forecasting at all stations in the EUMENA region, but might be sufficient in Australia, the western United States, and parts of southern America depending on the critical deviation threshold chosen by the user based on technical and economic considerations.

Deviations are at least 2 times lower from 10 to 15 h true solar time (TST) than in other periods of the day for most stations. Additionally, for continental average and maritime clean types, there is only around 10% of hours with an AOD deviation leading to at least a 20% DNI deviation during the most energetic period of the day.

PERFORMANCE OF A GLOBAL STATE-OF-THE-ART NWP AEROSOL MODEL. Using the scheme described in Fig. 1 the ECMWF/MACC AOD forecasts out of the 0000 UTC run for day 2 (25–48-h lead time) are validated against AERONET measurements (Fig. 7). It has to be noted that there are spatiotemporal errors due to the comparison of the model grid average versus a point measurement. On the other hand, this is exactly the user's approach when applying a global NWP model to forecast DNI for solar power plant sites of a maximum size of 1–2 km^2. From the user's point of view there might be a discrepancy between a local measurement and the model forecast—whether this is related to any model error or unresolved sub-grid-scale variability is not relevant for users. Therefore, this validation approach is consistent with the potential use of such forecasts.

Rather low relative DNI RMS and bias are obtained: generally, values between 5% and 15% are

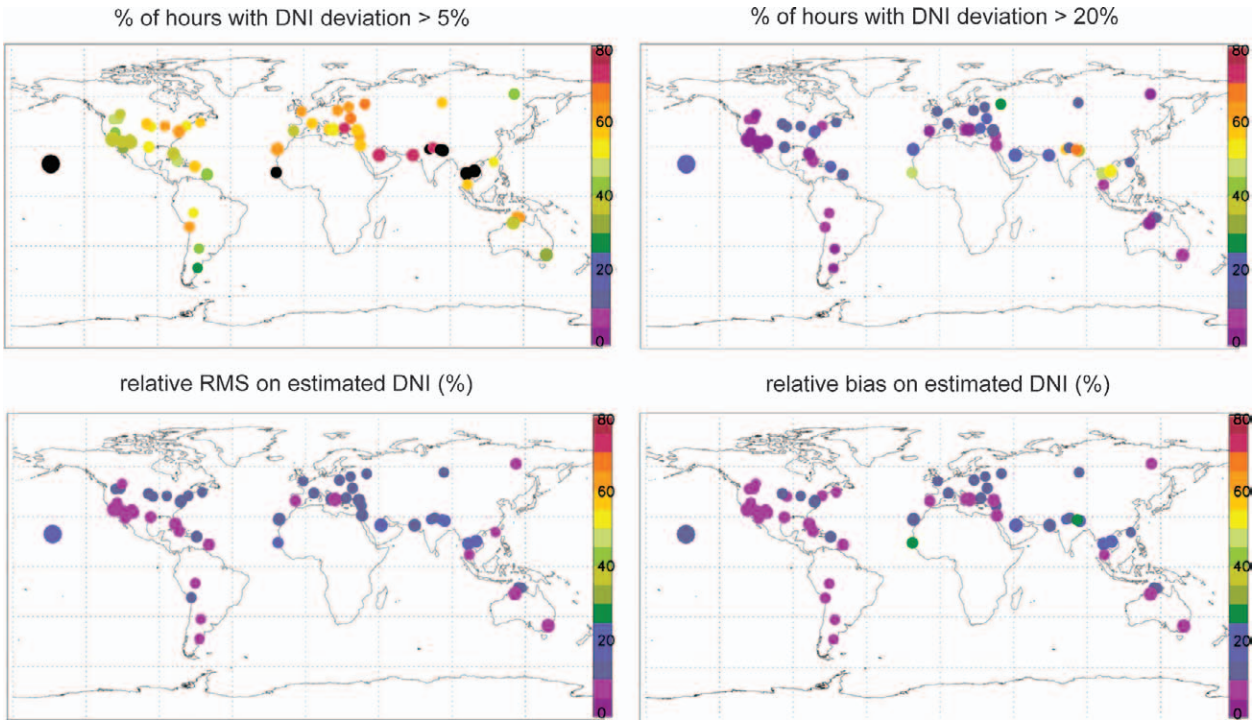

Fig. 7. ECMWF/MACC forecast (hourly comparison, bilinear interpolation) performance at AERONET stations. The maximum number of hours is 942, the minimum is 101, and the disk size is proportional to (1 + number of hours/maximum number). Black points correspond to deviations higher than 80%.

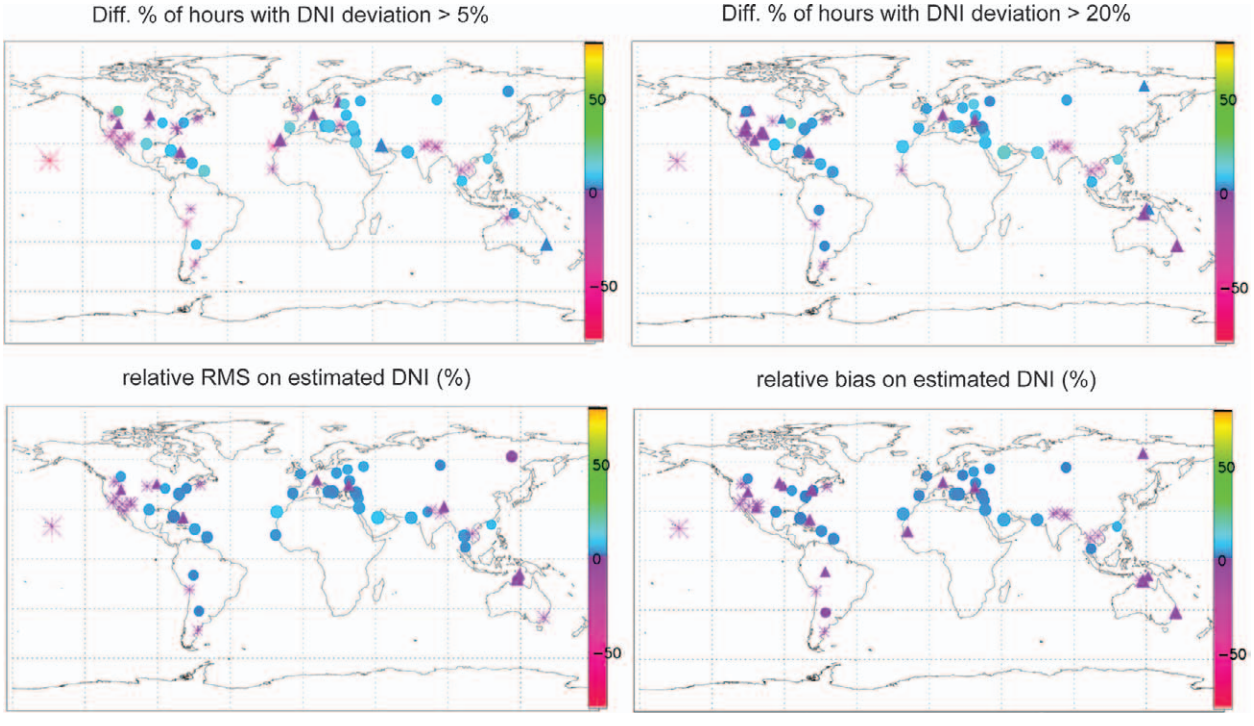

Fig. 8. Differences between parameters obtained with ECMWF/MACC forecasts and with 2-day persistence. Triangles correspond to stations where both accuracies are similar within a 2% range for the percentage of hours. Disks are made if the percentage is higher than 2%, while stars represent a percentage less than −2%. For RMS and bias this separation is made with a 1% threshold.

found, although higher deviations are observed in Southeast Asia and at the west coast of Africa. The percentage of hours with a ΔDNI larger than 20% is also low, especially in the western United States, where it is less than 10%. This percentage remains generally less than 20% in the eastern United States, in Europe as well as in southern America and Australia. Remarkably higher percentages are obtained for all stations if the critical ΔDNI is set to 5%. Some stations—in black—even exhibit percentages higher than 80%.

The error measures as a function of true solar time have similar shapes as those observed for the 2-day persistence. The percentage of hours is highly hourly sensitive, but being less in hours with larger DNI. Values around 10% are found between 10 and 14 h TST and reach 25% at 6 or 18 h TST for the 20% criterion. For the 5% criterion they are around 45% between 10 and 14 h TST and reach 75% at 6 or 18 h TST.

Error measures of the ECMWF/MACC forecast are also compared to that of the 2-day persistence approach (Fig. 8). Positive difference of the individual error measures correspond to stations where ECMWF/MACC performs better, while negative values represent AERONET stations when the 2-day persistence is advantageous. ECMWF/MACC performs better at most stations, especially in Europe. The performance in the western United States is generally very good (Fig. 7); therefore, it is not significant that the 2-day persistence performs better there. In eastern Asia, as well as in western Africa, the ECMWF/MACC forecast is not fully able to describe the regional features leading to statistical measures worse than the 2-day persistence. That might be due to a rapid Asian industrialization, which is not yet taken into account in most emission databases, and to a yet-incomplete knowledge of dust mobilization and transport.

CONCLUSIONS. An assessment of requirements on aerosol forecasting capabilities with special respect to solar energy usage has been made. Critical thresholds of AOD deviation are generated and used in statistics of exceedance hours, when the AOD deviation is relevant with respect to a certain maximum DNI deviation accepted. This measure takes into account that the relative deviation on the solar energy received at the power plant is a nontrivial function of ΔAOD being reflected in radiative transfer theory. The same ΔAOD value in a specific hour of the day can be of relevance or not, depending on the solar position and the actual AOD itself. This complex dependency is the explanation why existing, classical AOD forecast verification against AERONET as, for example, in Morcrette et al. (2011) is indeed meaningful, but not sufficient for solar energy applications.

In the paper results for 5% and 20%, DNI deviations are shown while the study was also performed for a 10% deviation. Nevertheless, it is expected that each user group will define their own acceptable DNI deviation, as this depends very much on specific design parameters of the chosen solar technology and actual economic conditions assumed in viability assessments of a specific power plant. Therefore, this paper presents both a strict and a loose criterion as a first orientation for the user community and as a justification of the design of future aerosol forecasting capabilities at the meteorological centers.

With exception of Southeast Asia, the influence of the AOD daily variation on hourly DNI deviations is small if the 20% DNI deviation criterion is assessed. This assumption cannot be made in most regions if a stricter DNI deviation criterion is applied. Additionally, lower DNI deviations are found during small solar zenith angles around noon in the most energetic phase of the day. Areas like Australia, the western United States, oceanic regions, and southern parts of South America can be treated with the persistence approach, but in all other regions this approach results in large numbers of exceedance hours also in the 20% DNI deviation criterion. Generally, the performance of the ECMWF/MACC forecast is better or equal to the 2-day persistence with the exception of some Asian and western African stations. A further reduction of forecast deviations especially in regions with air pollution or large dust concentrations is recommended. This holds especially if larger shares of regional electricity production are generated from concentrating solar power as nowadays in Spain. Such a situation will result in significantly higher accuracy requirements on a regional scale in order to provide an accurate forecast of the solar electricity production as input to an electricity grid stabilization procedure.

Improvements within the description of dust emissions are ongoing at the ECMWF, resulting in improved forecasts that may benefit the solar industry applications. Within the GMES Atmosphere Service preparations during the MACC-II project, further development towards a modal aerosol representation, improved emission databases, and the use of other satellite observations than MODIS in the data assimilation scheme is foreseen. Especially, the assimilation of MODIS Deep Blue aerosol optical depth over desert areas (Hsu et al. 2004, 2006; Ginoux et al. 2012) and

of Cloud-Aerosol Lidar with Orthogonal Polarization (CALIOP)-derived aerosol vertical distribution is expected to improve the model aerosol forecasts with direct benefit to the solar energy user community.

ACKNOWLEDGMENTS. This work has been funded by the European Commission within the EU Seventh Research Framework Program's project Monitoring Atmospheric Composition and Climate (MACC) under Contract 218793. Thanks to the data policy of European Commission's Global Monitoring for Environment and Security (GMES) initiative the ECMWF/MACC NRT run is freely available on the MACC project website (www.gmes-atmosphere.eu). B. Holben and his collaborators are thanked for setting up and maintaining the AERONET station network. Finally, we acknowledge the work performed by the LibRadtran development team lead by B. Mayer and A. Kylling.

REFERENCES

Benedetti, A., and Coauthors, 2009: Aerosol analysis and forecast in the European Centre for Medium-Range Weather Forecasts Integrated Forecast System: 2. Data assimilation. *J. Geophys. Res.,* **114,** D13205, doi:10.1029/2008JD011115.

Beyer, H.-G., C. Costanzo, and D. Heinemann, 1996: Modifications of the Heliosat procedure for irradiance estimates from satellite images. *Sol. Energy,* **56,** 207–212.

Breitkreuz, H., M. Schroedter-Homscheidt, T. Holzer-Popp, and S. Dech, 2009: Short-range direct and diffuse irradiance forecasts for solar energy applications based on aerosol chemical transport and numerical weather modeling. *J. Appl. Meteor. Climatol.,* **48,** 1766–1779.

Cano, D., J. Monget, M. Albuisson, H. Guillard, N. Regas, and L. Wald, 1986: A method for the determination of the global solar radiation from meteorological satellite data. *Sol. Energy,* **37,** 31–39.

Ginoux, P., J. M. Prospero, T. E. Gill, N. C. Hsu, and M. Zhao, 2012: Global-scale attribution of anthropogenic and natural dust sources and their emission rates based on MODIS Deep Blue aerosol products. *Rev. Geophys.,* **50,** RG3005, doi:10.1029/2012RG000388.

Hess, M., P. Koepke, and I. Schult, 1998: Optical Properties of Aerosols and Clouds: The software package OPAC. *Bull. Amer. Meteor. Soc.,* **79,** 831–844.

Holben, B. N., and Coauthors, 1998: AERONET—A federated instrument network and data archive for aerosol characterization. *Remote Sens. Environ.,* **66,** 1–16.

Hsu, N. C., S.-C. Tsay, M. King, and J. R. Herman, 2004: Aerosol properties over bright-reflecting source regions. *IEEE Trans. Geosci. Remote Sens.,* **42,** 557–569.

——, ——, ——, and ——, 2006: Deep Blue retrievals of Asian aerosol properties during ACE-Asia. *IEEE Trans. Geosci. Remote Sens.,* **44,** 3180–3195.

Huneeus, N., and Coauthors, 2011: Global dust model intercomparison in AeroCom phase I. *Atmos. Chem. Phys.,* **11,** 7781–7816, doi:10.5194/acp-11-7781-2011.

Klein, S. A., and Coauthors, cited 2010: TRNSYS 17: A Transient System Simulation Program. [Available online at http://sel.me.wisc.edu/trnsys.]

Klinker, E., F. Rabier, G. Kelly, and J.-F. Mahfouf, 2000: The ECMWF operational implementation of four-dimensional variational assimilation. III: Experimental results and diagnostics with operational configuration. *Quart. J. Roy. Meteor. Soc.,* **126,** 1191–1215.

Kraas, B., R. Madlener, B. Pulvermüller, and M. Schroedter-Homscheidt, 2010: Viability of a concentrating solar power forecasting system for participation in the Spanish electricity market. *Proc. SolarPaces 2010,* Perpignan, France, IEA SolarPaces programme and CNRS-PROMES.

——, M. Schroedter-Homscheidt, R. Madlener, and B. Pulvermüller, 2011: Economic assessment of a concentrating solar power forecasting system for participation in the Spanish electricity market. *Sol. Energy,* in press.

Kylling, A., and Coauthors, 2005: Spectral actinic flux in the lower troposphere: Measurement and 1-D simulations for cloudless, broken cloud and overcast situations. *Atmos. Chem. Phys.,* **5,** 1975–1997.

Lara-Fanego, V., J.-A. Ruiz-Arias, D. Pozo-Vázquez, F. J. Santos-Alamillos, and J. Tovar-Pescador, 2012: Evaluation of the WRF model solar irradiance forecasts in Andalusia (southern Spain). *Sol. Energy,* **86,** 2200–2217.

Mahfouf, J.-F., and F. Rabier, 2000: The ECMWF operational implementation of four-dimensional variational assimilation. II: Experimental results with improved physics. *Quart. J. Roy. Meteor. Soc.,* **126,** 1171–1190.

Mayer, B., and A. Kylling, 2005: Technical note: The libRadtran software package for radiative transfer calculations—Description and examples of use. *Atmos. Chem. Phys.,* **5,** 1855–1877, doi:10.5194/acp-5-1855-2005.

Ministerio de Industria, Turismo y Comercio, 2007: Real Decreto 661/2007, de 25 de Mayo, por el que se regula la actividad de producción de energía eléctrica en régimen especial. *Boletín Oficial des Estado,* No. 126, Agencia Estatal Boletín Oficial del Estado, 22 846–22 886. [Available online at www.boe.es/buscar/doc.php?id=BOE-A-2007-10556.]

Morcrette, J.-J., and Coauthors, 2009: Aerosol analysis and forecast in the European Centre for Medium-Range Weather Forecasts Integrated Forecast System: Forward modeling. *J. Geophys. Res.,* **114,** D06206, doi:10.1029/2008JD011235.

——, A. Benedetti, L. Jones, J. W. Kaiser, M. Razinger, and M. Suttie, 2011: Prognostic aerosols in the ECMWF IFS: MACC vs GEMS aerosols. European Centre for Medium-Range Weather Forecasts Tech. Memo. 659, 32 pp. [Available online at www.ecmwf.int/publications/library/do/references/show?id=90354.]

Pulvermüller, B., M. Schroedter-Homscheidt, B. Pape, J. Casado, and K.-J. Riffelmann, 2009: Analysis of the requirements for a CSP energy production forecast system. *Proc. SolarPaces 2009,* Berlin, Germany, German Aerospace Center.

Rabier, F., H. Jbinen, E. Klinker, J.-F. Mahfouf, and A. Simmons, 2000: The ECMWF operational implementation of four-dimensional variational assimilation. I: Experimental results with simplified physics. *Quart. J. Roy. Meteor. Soc.,* **126,** 1143–1170.

Remer, L. A., and Coauthors, 2005: The MODIS aerosol algorithm, products, and validation. *J. Atmos. Sci.,* **62,** 947–973.

Rigollier, C., M. Lefèvre, and L. Wald, 2004: The method Heliosat-2 for deriving shortwave solar radiation from satellite images. *Sol. Energy,* **77,** 159–169.

Shiobara, M., and S. Asano, 1994: Estimation of cirrus optical thickness from sun photometer measurements. *J. Appl. Meteor.,* **33,** 672–681.

Stamnes, K., S.-C. Tsay, W. Wiscombe, and K. Jayaweera, 1988: Numerically stable algorithm for discrete–ordinate–method radiative transfer in multiple scattering and emitting layered media. *Appl. Opt.,* **27,** 2502–2509.

Thomalla, E., P. Köpke, H. Müller, and H. Quenzel, 1983: Circumsolar radiation calculated for various atmospheric conditions. *Sol. Energy,* **30,** 575–587.

Wagner, M. J., and P. Gilman, 2011: Technical manual for the SAM Physical Trough Model. NREL Tech. Rep. NREL/TP-5500-51825, 124 pp. [Available online at https://sam.nrel.gov/webfm_send/106.]

Wittmann, M., H. Breitkreuz, M. Schroedter-Homscheidt, and M. Eck, 2008: Case studies on the use of solar irradiance forecast for optimized operation strategies of solar thermal power plants. *IEEE J. Sel. Top. Appl. Earth Obs. Remote Sens.,* **1,** 18–27, doi:10.1109/JSTARS.2008.2001152.

WMO, 2010: Measurement of radiation. WMO guide to meteorological instruments and methods of observation, WMO-No. 8., I.7-1–I.7-41. [Available online at www.wmo.int/pages/prog/www/IMOP/CIMO-Guide.html.]

APPENDIX: AERONET STATIONS. This appendix provides an overview about aerosol types selected for AERONET stations used in the study. Generally, a "continental average" type has been assumed, while some AERONET stations are classified as being of type "urban" (Table A1), "desert" (Table A2), and "maritime clean" (Table A3).

Table A1. AERONET stations with urban type selected.

Station	Latitude	Longitude	Station	Latitude	Longitude
ATHENS-NOA	37.988°	23.775°	Hong Kong PolyU	22.303°	114.18°
Barcelona	41.386°	2.117°	Jaipur	26.906°	75.806°
Brasilia	–15.917°	–47.9°	Lahore	31.542°	74.325°
Cairo EMA	30.081°	31.29°	London-UCL-UAO	51.524°	–0.131°
Cairo University	30.026°	31.207°	Manila Observatory	14.635°	121.078°
Hong Kong Hok Tsui	22.21°	114.258°	Mexico City	19.334°	–99.182°
Hong Kong PolyU	22.303°	114.18°	Monterey	36.593°	–121.855°
Moscow MSU MO	55.7°	37.51°	Philadelphia	40.036°	–75.005°
Nairobi	–1.339°	36.865°	Pune	18.537°	73.805°
New Delhi	28.63°	77.175°	Rome Tor Vergata	41.84°	12.647°
Osaka	34.651°	135.591°	Santiago	–33.49°	–70.717°
Paris	48.867°	2.333°	Sao Paulo	–23.561°	–46.735°
Seoul SNU	37.458°	126.951°	Taichung	24.106°	120.491°
Singapore	1.298°	103.78°	Taipei CWB	25.03°	121.5°
Toronto	43.97°	–79.47°			

Table A2. AERONET stations with desert type selected.					
Station	**Latitude**	**Longitude**	**Station**	**Latitude**	**Longitude**
Agoufou	15.345°	–1.479°	Guadeloup	16.333°	–61.5°
Al Dhafra	24.254°	54.55°	Hamim	22.967°	54.3°
Andros Island	24.7°	–77.8°	IER Cinzana	13.278°	–5.934°
Banizoumbou	13.541°	2.665°	Ilorin	8.32°	4.34°
Barbados	13.15°	–59.617°	Kanpur	26.513°	80.232°
Bidi Bahn	14.06°	–2.45°	La Parguera	17.97°	–67.045°
Cape San Juan	18.384°	–65.62°	Mussafa	24.372°	54.467°
Capo Verde	16.733°	–22.935°	Ouagadougou	12.2°	–1.4°
Dahkla	23.717°	–15.95°	Paddockwood	53.5°	–105.5°
Dakar	14.394°	–16.959°	Solar Village	24.907°	46.397°
Dhabi	24.481°	54.383°	Surinam	5.8°	–55.2°
Djougou	9.76°	1.599°			

Table A3. AERONET stations with maritime clean type selected.					
Station	**Latitude**	**Longitude**	**Station**	**Latitude**	**Longitude**
Amsterdam Island	–37.81°	77.573°	MCO-Hanimaadhoo	6.776°	73.183°
Ascension Island	–7.976°	–14.415°	Mauna Loa	19.539°	–155.578°
Azores	38.53°	–28.63°	Midway Island	28.21°	–177.378°
Bermuda	32.37°	–64.696°	Nauru	–0.521°	166.916°
Coconut Island	21.433°	–157.79°	Okinawa	26.357°	127.768°
Crozet Island	–46.435°	51.85°	Praia	14.947°	–23.484°
Graciosa	39.091°	–28.03°	Prospect Hill	32.37°	–64.696°
Guam	13.431°	144.801°	Reunion St Denis	–20.883°	55.483°
Izana	28.309°	–16.499°	Ragged Point	13.165°	–59.432°
Kaashidhoo	4.965°	73.466°	Santa Cruz Tenerife	28.473°	–16.247°
La Laguna	28.482°	–16.321°	Tahiti	–17.577°	–149.606°
Lanai	20.735°	–156.922°	Tenerife	28.033°	–16.633°
MALE	4.192°	73.529°	Tudor Hill	32.264°	–64.879°